ROZPRAWY INŻYNIERSKIE • ENGINEERING TRANSACTIONS • 36, 3, 471–486, 1988
Polska Akademia Nauk • Instytut Podstawowych Problemów Techniki

NUMERICAL ANALYSIS OF BEAMS AND FRAMES WITH STRAIN-SOFTENING MATERIALS

T. ŁODYGOWSKI (POZNAŃ)*)

The present study shows the softening post-peak deflection behaviour of beams and frames for cracking reinforced concrete materials. The layered finite elements are used in the analysis. Concrete exhibits strain-softening effects in tension and compression and the steel reinforcement is assumed to be elastic-plastic. The bond slip of reinforcement is neglected but still it is shown that the model satisfactorily approximates the existing experimental tests. The arc-length method which seems to be very general even for snap-through and snap-back structural behaviour, is used in numerical analysis.

1. Introduction

A structure with both physical and geometrical nonlinearities can sometimes exhibit a softening response in which the load parameter declines with increasing displacement after its peak value has been reached. For post buckling analysis of elastic structures or for concrete and reinforce-concrete (strain-softening materials) structures such softening behaviour is typical.

Recently great attention has been focussed on finding general solution algorithms for the nonlinear behaviour of structures. From the numerical point of view the whole structural response after the limit or bifurcation point has been reached is of particular interest (snap-through or snap-back).

It is convenient to present the behaviour of the structure as a path in the space of the displacement vector components $\mathbf{q}$ and load parameter λ (for one-parametric cases) — Fig. 1. When using the typical load control incremental process, it fails for the max value of λ when singularity of the stiffness matrix appears. For many practical problems when only the snap--thorugh in structural response is observed, the components of displacements are chosen as control parameters. In such cases we have displacement

*) Fulbright Scholar at Northwestern University, on leave from the Technical University of Poznań, Poland.

control algorithms [1–4]. Even these procedures cannot overcome the difficulty of the snap-back phenomenon. However, there are some proposition e.g. BERGAN'S stiffness parameter [5], KRÖPLIN'S and DRINKLER'S creep type

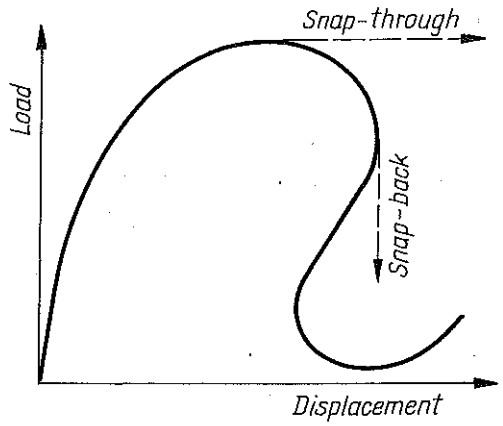

FIG. 1.

strategy [6, 7] which improve the efficiency of nonlinear analysis. WEMPNER'S and RIKS' ideas [8, 9], developed by RAMM [10] and CRISFIELD [11–14] based on the arc-length parameter, overcome the above difficulty and recently seems to be the most general and the most powerful in the post-critical analysis of structures of any type. This method will be adopted here for the analysis of structures made of strain-softening materials. All of these methods with their extensions are summarized in detail in the study [4].

In this work the softening post-peak deflection relationships for cracking reinforced-concrete beams and frames are analysed by layered finite elements. This type of element, studied previously in [15] but with geometric nonlinearities which are now omitted, seems from the engineering and design viewpoint to be accurate enough and has the additional advantage that it permits the numerical analysis of complex structures with a small number of degrees of freedom. The method can easily be extended to geometrically nonlinear cases by using, for example, a convected formulation as presented in [22] or [15].

2. STATEMENT OF THE PROBLEM

Let us consider beams or frames made of softening material (e.g. concrete) possibly reinforced by elastic-plastic bars. The assumption of the bending theory are used and the bond slip of reinforcement is neglected. In numerical examples the softening material (concrete) is assumed to exhibit

strain-softening in both tension and compression. We will use the "smeared model" of material [16, 17], and we will not discuss the problems of crack growth and propagation and localization effects [18]. Under these assumptions we are allowed to formulate the laminated finite element. Details are presented in Appendix A. Moreover, the omission of shear deformations makes it possible to discuss the constitutive law in one-dimensional form.

The numerical results reached in this study are based on the implementation of the arc-length method. Some of them show the influence of finite element discretization on the final limit loads.

3. Constitutive law for layer

An uniaxial stress-strain relation will be used for the concrete with the approximate piece-wise linear diagram shown in Fig. 2a and with strain-softening effects in both tension and compression.

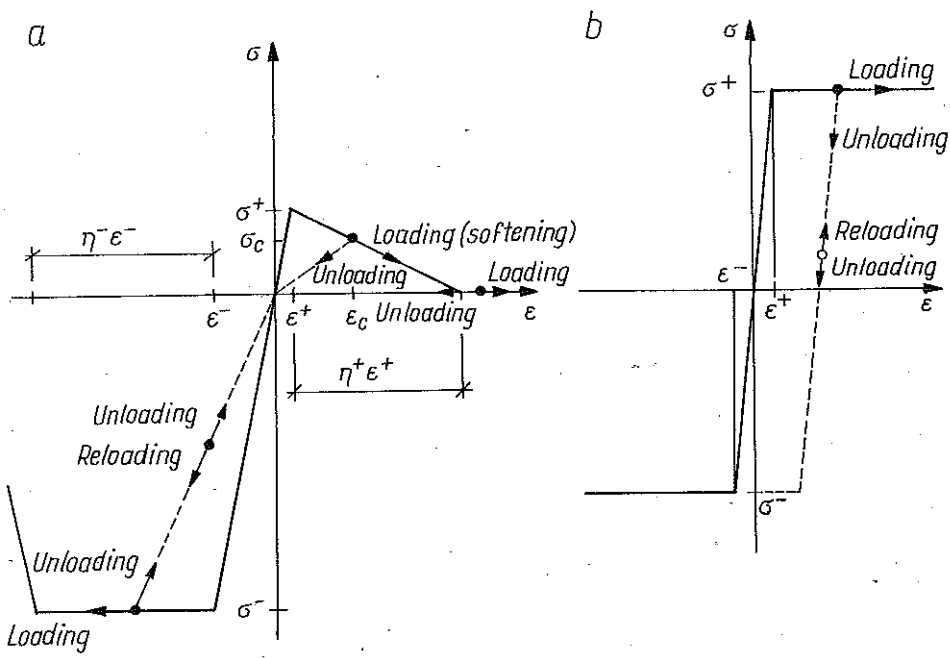

Fig. 2. a) concrete, b) steel.

3.1. Concrete

The unloading diagram Fig. 2a assumed here is the straight line passing through the origin. Its slope is equal to the secant modulus at the maximum strain reached. This is a simplification of concrete behaviour. The softening in tension and the size of the plateau in compression are characterized by the parameters η^+, η^-. One of the most important points in incrementally iterative procedures is the proper choice of the constitutive state of each layer and adopting the value of E_τ. The problem becomes complicated when a layer unloads so that $\dot{\sigma}$ changes sign. The constitutive relation is fully described using the following parameters: E_τ, ε^+, ε^-, σ^+, σ^-, η^+, η^-. In addition a vector which stores the indicators of each layer's constitutive state is introduced (e.g. IND = 0 for loading of IND = 1 for unloading).

3.2. Steel

The adopted constitutive law for steel elements is presented in Fig. 2b. We assume the ideally elastic-plastic behaviour. All possible modifications of the constitutive state of each layer that appear during the incremental process are expressed in Fig. 2 and are used in finite element code. The nonlinear constitutive relation is the only reason for nonlinear structural behaviour so the proper description of unloading-reloding states of laminas and the proper limits modifications (e.g. σ_c, ε_c) are extremly important.

4. The method of solution

Before we present the flow-chart for solving the incrementally formulated physical problem, let us present some basic ideas connected with the arc-length method used in the analysis.

4.1. Arc-length method

The governing equilibrium equation where the load level λ is treated as a variable can be expressed as

$$\mathbf{g}(\mathbf{q}) = \mathbf{f}^{\text{int}}(\mathbf{q}) - \lambda \mathbf{p}, \tag{4.1}$$

where $\mathbf{f}^{\text{int}}$ is the vector of internal forces, $\mathbf{g}$ is the out of balance force vector and both depend on the current displacements $\mathbf{q}$; $\mathbf{p}$ denotes a fixed total load vector. Since we assume the scalar λ as a variable, the additional constraint equation is required to fix the increments of displacements. For this purpose we choose the load parameter to lie on the $(N+1)$-dimension hyper-sphere given by:

$$\Delta \mathbf{q}_i^T \Delta \mathbf{q}_i + \alpha \Delta \lambda_i^2 \mathbf{p}^T \mathbf{p} = \Delta l^2, \tag{4.2}$$

where Δq_i and $\Delta \lambda_i$ are the vector of incremental displacements and load parameter at i-th iteration respectively, Δl is the arc-length at the current step. Following Crisfield's suggestion, we adopt the above equation

$$\Delta \mathbf{q}_i^T \Delta \mathbf{q}_i = \Delta l^2, \tag{4.3}$$

so we will not discuss the meaning of the scaling parameter α.

Let us introduce the following notation in which the subscript 0 describes the displacements ($\mathbf{q}_0$), internal forces ($\mathbf{f}_0^{\text{int}}$) on the load level ($\lambda_0$) in the equilibrium state at the beginning of increment. It means that for perfect convergence

$$\mathbf{f}_0^{\text{int}}(\mathbf{q}_0) = \lambda_0 \mathbf{p}. \tag{4.4}$$

The iterative procedure involves

$$\begin{aligned} \lambda_{i+1} &= \lambda_0 + \Delta\lambda_{i+1} = \lambda_i + \delta\lambda_i, \\ \mathbf{q}_{i+1} &= \mathbf{q}_0 + \Delta\mathbf{q}_{i+1} = \mathbf{q}_i + \boldsymbol{\delta}_i, \\ \Delta\mathbf{q}_{i+1} &= \Delta\mathbf{q}_i + \boldsymbol{\delta}_i, \end{aligned} \tag{4.5}$$

where the subscripts denote the number of iterations, and for simplicity the acceleration parameter is omitted in the formulas. We are looking for the equilibrium state in the new configuration where

$$\mathbf{g}(\lambda + \Delta\lambda, \mathbf{q}) = \mathbf{f}^{\text{int}}(\mathbf{q}) - (\lambda + \Delta\lambda)\mathbf{p} = \mathbf{g}(\lambda) - \Delta\lambda\mathbf{p} = \mathbf{0}. \tag{4.6}$$

The $mN-R$ technique assumes that the tangent stiffness matrix $\mathbf{K}$ is formed at the beginning of the increment and remains fixed for all iterations. The additional displacement is obtained by

$$\boldsymbol{\delta}_i = -K^{-1}\mathbf{g}(\lambda_i + \delta\lambda_i) = \hat{\boldsymbol{\delta}}_i + \delta\lambda_i \boldsymbol{\delta}_T, \tag{4.7}$$

where

$$\hat{\boldsymbol{\delta}}_i = -\mathbf{K}^{-1}\mathbf{g}(\lambda_i) \quad \text{and} \quad \boldsymbol{\delta}_T = \mathbf{K}^{-1}\mathbf{p}. \tag{4.8}$$

When using $mN-R$, we see that $\boldsymbol{\delta}_T$ is found just once at the beginning increment and only $\boldsymbol{\delta}_i$ is modified in the iterative process. Assuming perfect convergence at the last increment, we obtain

$$\boldsymbol{\delta}_0 = \Delta\lambda, \boldsymbol{\delta}_T. \tag{4.9}$$

We notice that the vector $\boldsymbol{\delta}_i$ Eq. (4.7) is fully defined only if $\delta\lambda_i$ is known. Substituting Eqs. (4.7) and (4.5) into Eq. (4.3) yields

$$a_1 \delta\lambda_i^2 + a_2 \delta\lambda_i + a_3 = 0, \tag{4.10}$$

where the coefficients are

$$
\begin{aligned}
a_1 &= \boldsymbol{\delta}_T^T \boldsymbol{\delta}_T, \\
a_2 &= 2\,(\Delta\mathbf{q}_i + \hat{\boldsymbol{\delta}}_i)^T \boldsymbol{\delta}_T, \\
a_3 &= \hat{\boldsymbol{\delta}}_i^T \hat{\boldsymbol{\delta}}_i + 2\Delta\mathbf{q}_i^T \hat{\boldsymbol{\delta}}_i.
\end{aligned} \tag{4.11}
$$

Among the two roots of Eq. (4.10) the appropriate one is chosen using the criterion which ensures an acute angle θ between $\Delta\mathbf{q}_i$ and $\Delta\mathbf{q}_{i+1}$. It generally leads to the one which is the closest root to the linear solution if both roots generate the positive value of $\cos\theta$. The second root is simply omitted and is not discussed any more.

It is assumed that the arc-length Δl is known at each increment. For the first increment the initial value of $\Delta\lambda_1$ is applied and it involves the first length as

$$
\Delta l = \Delta\lambda_1 \sqrt{\boldsymbol{\delta}_T^T \boldsymbol{\delta}_T}\,. \tag{4.12}
$$

The magnitude of the next incremental length is changed as a function of number of iterations required at the previous increment of load and the previous value of Δl. So the first value of incremental load for new step is found as

$$
\Delta\lambda_1 = \pm \Delta l / \sqrt{\boldsymbol{\delta}_T^T \boldsymbol{\delta}_T}\,. \tag{4.13}
$$

where the sign follows the sign of $\det \mathbf{K}$ in our analysis.

4.2. Solution by finite elements with arc-length method implemented

The incremental process is carried out according to the arc-length method previously shown. The main steps of the algorithm are briefly stated as follows:

1. Read the input data — structure geometry, parameters of constitutive law.
2. Initialize.
3. Loop on loading steps.
4. Formulate the stiffness matrix of a structure $\mathbf{K}$.
5. Find the inverse stiffness matrix $\mathbf{K}$ (in fact factorization).
6. Loop on iterations where both increments of the load parameter $\delta\lambda$ and increments of the displacement vector $\Delta\mathbf{q}$ are iterated.
7. For each point check the loading-unloading conditions (constitutive law code). Solve the system of equilibrium equations to obtain the new nodal displacements.
8. Check the convergence criterion [5]. Usually the criterion is, according to the maximum value of residual forces in each node, $\|R_i\| < \vartheta \quad i = 1, \ldots$ n.d.f., or $\left|\sum_i \delta_{iN}^2 / \sum_i \delta_{ip}^2 - 1\right| < \vartheta$ where δ_{iN}, δ_{ip} are new and previous

values of i-th displacement components, ϑ is the chosen tolerance. If the criterion is not met, go to step 6.

9. Calculate the answer of the system at the end of the incremental step. Print the results. Return to step 3 and start the next loading step after the updating of all values.

5. Numerical examples

5.1. *Concrete beam*

Consider a simply supported beam Fig. 3 in which all layers have the same softening properties. The values of the parameters that describe the constitutive law are: $E = 30.0$ GPa, $\varepsilon^+ = 0.000133$, $\varepsilon^- = -0.00137$, $\sigma^+ = 4.0$ MPa, $\sigma^- = -41.0$ MPa, $\eta^+ = 8.0$, $\eta^- = 20.0$.

The cross section of the beam (its depth) is divided into 12 layers, and because of the symmetry only half of the beam is analysed using 2, 4 and 8 elements. The obtained results that present the y displacement of point A (midspan) versus the load parameter λ are plotted in Fig. 4. These results are very sensitive to the chosen element size. When the element size decreases, a sharper drop of the load is observed. It is due to strain localization in the midspan of a beam. For the smaller number of elements under the averaging of strains adopted here the strain localization effect is not so strong.

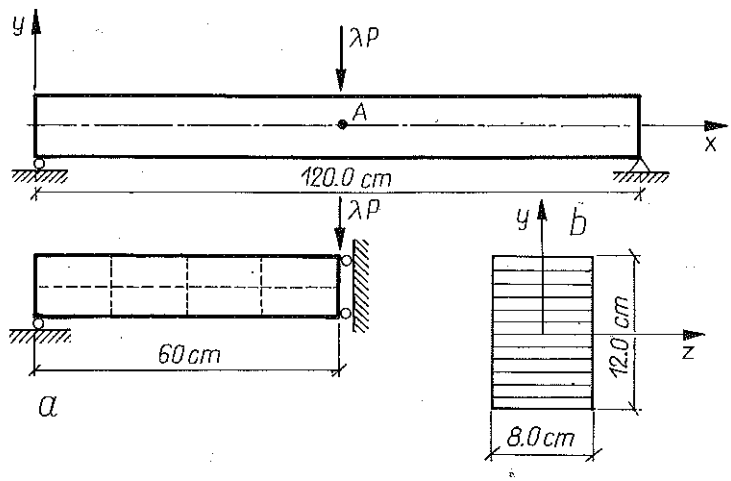

Fig. 3.

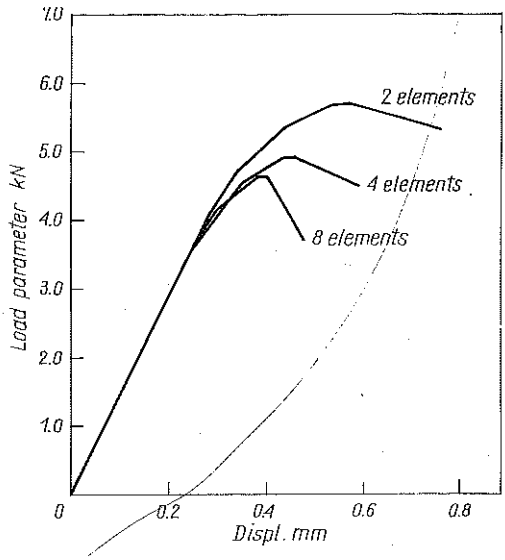

FIG. 4.

5.2. Reinforced concrete beam

In the beam Fig. 5 the reinforcement bars are treated as additional laminas with the steel properties, having the cross section of the same value as the bars. In this case we have 13 layers. The properties which are assumed for the analysis are expressed by the following parameters: for concrete $E = 30.0$ GPa, $\varepsilon^+ = 0.000133$, $\varepsilon^- = -0.00137$, $\sigma^+ = 4.0$ MPa, $\sigma^- = -41.0$ MPa, $\eta^+ = 8.0$, $\eta^- = 20.0$, and for steel $E = 200.0$ GPa, $\varepsilon^+ = -\varepsilon^- = 0.002$, $\sigma^+ = -\sigma^- = 40.0$ kN/cm^2. Figure 6 presents the results for

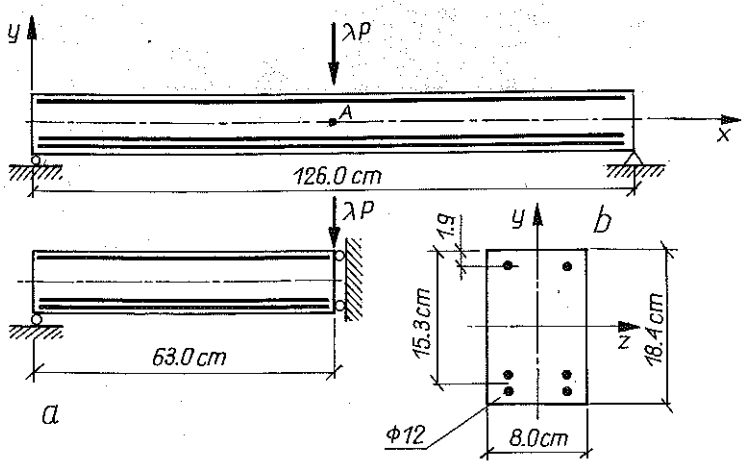

FIG. 5. a) structure, b) cross-section.

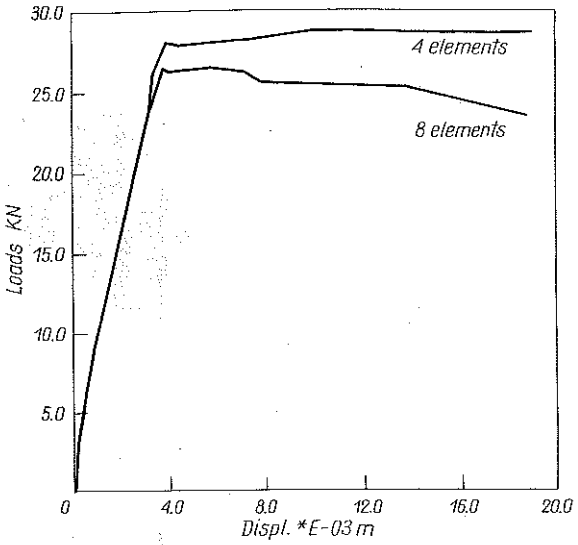

FIG. 6.

4 and 8 elements used in the numerical analysis. Like in the previous case this figure exhibits the same effect due to the element size. Figure 7 shows the stress distribution in the element, the closest one to the midspan, obtained numerically in the computations. It also shows the corresponding level of applied loads.

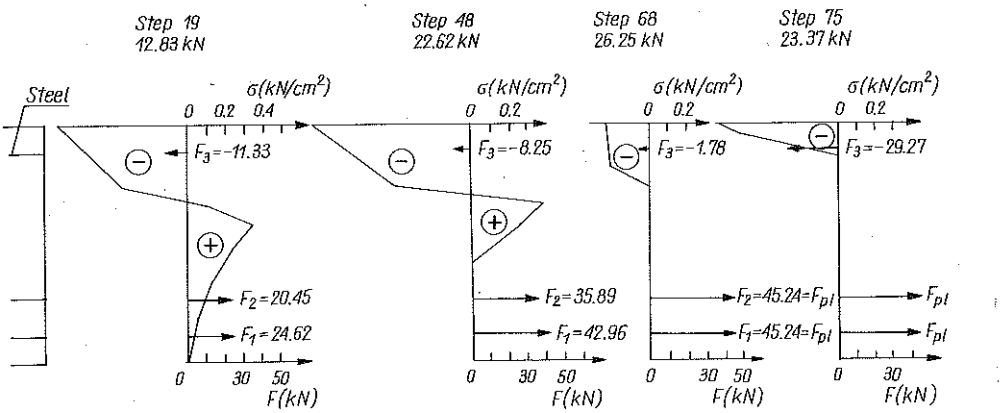

FIG. 7.

5.3. *Reinforced frame*

The frame Fig. 8 which is analysed reflects the experiment made by CRANSTON [20]. He tested the portal frame symmetrically loaded. In general

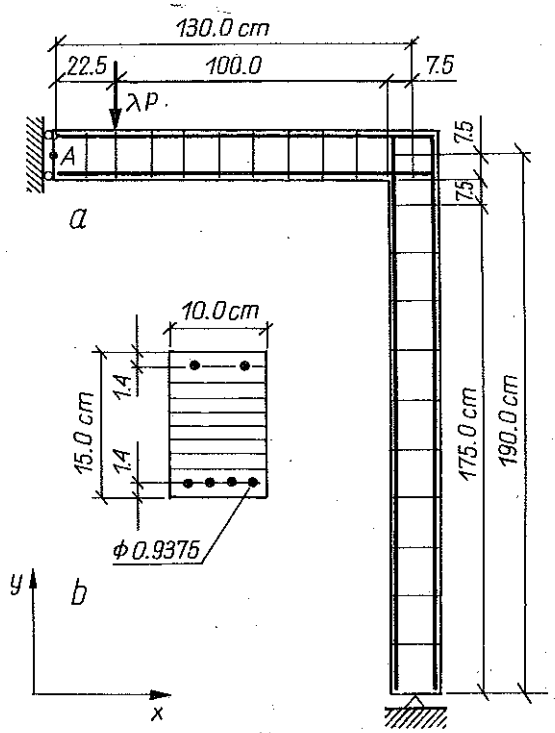

FIG. 8. a) structure, b) cross-section.

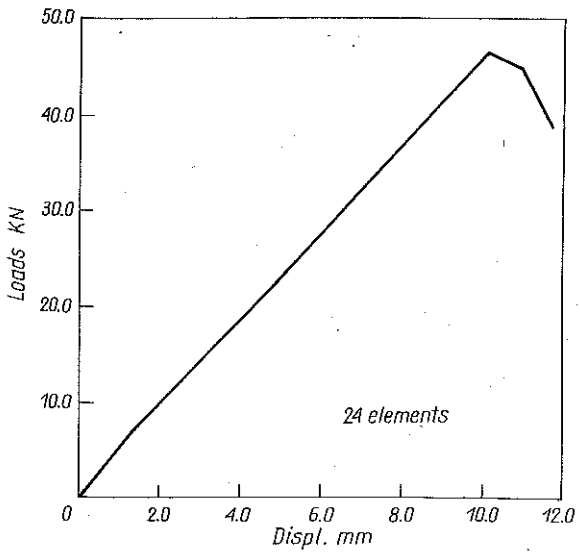

FIG. 9.

the failure mode of the frame need not be symmetric. Cranston's calculations show that bending moments taken from the experimental data in fact are symmetric. Therefore, for the numerical analysis we consider only one-half of the frame.

Data adopted for the material description are as follows: for conrete $E = 25.5$ GPa, $\varepsilon^+ = 0.0001$, $\varepsilon^- = -0.0014$, $\sigma^+ = 2.55$ MPa, $\sigma^- = -35.7$ MPa, $\eta^+ = 15.0$, $\eta^- = 30.0$, and for steel $E = 200.0$ GPa, $\varepsilon^+ = -\varepsilon^- = 0.002$, $\sigma^+ = -\sigma^- = 400.0$ MPa. The load-y displacement of point A relation is plotted in Fig. 9. The limit load obtained in the analysis agrees with experimental results.

6. Conclusions

The present study provides an efficient discretization procedure using the layered finite element approach. The iteration method, based on the arc-length concept, which is usually applied for elastic structures with geometrical nonlinearities, allows for a successful analysis of structures made of softening materials.

The softening post-peak behaviour of load-deflection diagrams can be explained in terms of the strain-softening behaviour of concrete. The presence of reinforcement stabilizes the behaviour of structures even if the advanced failure states appear in concrete layers.

The adopted numerical procedures show good convergence and in spite of previously reported difficulties [14] can be used for the analysis of physically nonlinear structures.

Appendix A. Finite element formulation

Let us introduce a finite element Fig. 10 which is a part of beam that each cross section is divided into n_l layers. The constitutive law for each layer can be different from the other as was discussed before. For the analysis of reinforce concrete structure, some layers can represent concrete and some the reinforcing bars.

The column matrices of element displacements and forces expressed in the local coordinate system are:

$$\mathbf{u} = \{u_1, v_1, \varphi_1, u_2, v_2, \varphi_2\}^T, \tag{A.1}$$

$$\mathbf{f} = \{N_1, S_1, M_1, N_2, S_2, M_2\}^T,$$

where u, v, φ, are axial displacement, transverse displacement and rotation of cross section and the subscripts 1 and 2 are referred to the adjacent

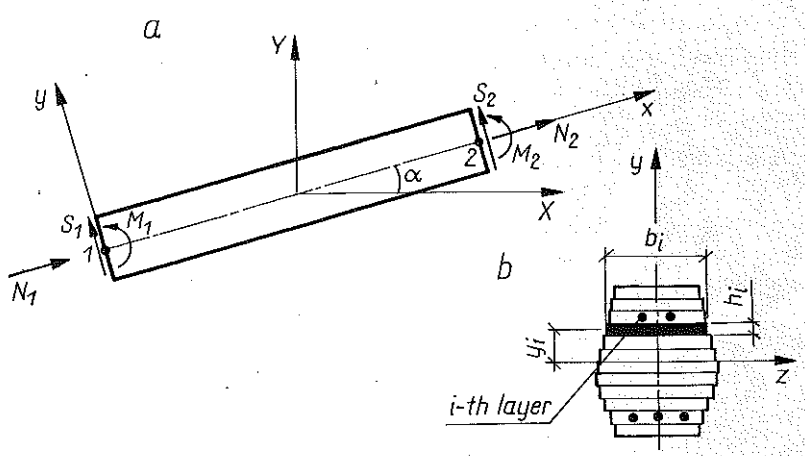

FIG. 10. a) Element in coordinate systems; b) cross-section.

cross sections at both ends of the element. The internal forces are due to the centroidal local axis x.

The strain at any point of the beam is

$$\varepsilon(x, y) = \partial u/\partial x, \tag{A.2}$$

where the displacement in axial direction is

$$u(x, y) = u(x, 0) - y\,\partial v(x, 0)/\partial x. \tag{A.3}$$

When using the following expressions describing axial and transverse displacements

$$u(x, 0) = (1-\xi)\,u_1 + \xi u_2, \tag{A.4}$$

$$v(x, 0) = (1-3\xi^2+2\xi^3)\,v_1 + (3\xi^2-2\xi^3)\,v_2 + L_e(\xi-2\xi^2+\xi^3)\,\varphi_1 + L_e(\xi^3-\xi^2)\,\varphi_2, \tag{A.5}$$

where $\xi = x/L_e$, L_e is the element length (Fig. 10) and substituting into Eqs. (A.3) and (A.2) we obtain the geometric equation in the form

$$\varepsilon(x, y) = \mathbf{B}\mathbf{u},$$
$$\mathbf{B} = 1/L_e\,\{-1;\ 6\eta(1-2\xi);\ 2L_e\eta(2-3\xi);\ 1;\ 6\eta(2\xi-1);\ 2L_e\eta(1-3\xi)\}, \tag{A.6}$$

where $\eta = y/L$.

Then classically, applying the virtual work principle to the beam element, we obtain

$$\mathbf{K}_e = \int_V \mathbf{B}^T E_T \mathbf{B}\,dV, \qquad \mathbf{f}^{\text{int}} = \int_V \mathbf{B}^T \boldsymbol{\sigma}\,dV, \tag{A.7}$$

where V is the element volume and E_T is the tangent elasticity modulus.

Along the axis x it is easy to integrate analytically and the integral over the cross section area is approximated by a sum over all layers $l = 1, \ldots, n$. It is assumed that the stresses are constant on the depth of a layer. The matrix $\mathbf{K}$ has to be transformed to the global coordinates in the form

$$\mathbf{K} = \mathbf{T}^T \mathbf{K}_e \mathbf{T}, \tag{A.8}$$

where the transformation matrix $\mathbf{T}$ has the following components: $T_{11} = T_{22} = T_{44} = T_{55} = \cos\alpha$, $T_{33} = T_{66} = 1.0$, $T_{12} = -T_{21} = T_{45} = -T_{54} = \sin\alpha$ and other T_{ij} are equal to 0.

Let us denote as follows:

$$\begin{aligned} Q &= \sum_{i}^{n_l} E_{Ti}\, b_i\, h_i, \\ R &= \sum_{i}^{n_l} E_{Ti}\, b_i\, h_i\, y_i, \\ S &= \sum_{i}^{n_l} E_{Ti}\, b_i\, h_i\, y_i^2, \end{aligned} \tag{A.9}$$

where b_i, h_i, y_i are width, depth, and centroidal y_i coordinate for the l-th layer, respectively. Then we simply obtain the transformed form of the element stiffness matrix as

$$K = \begin{bmatrix} K_{11} & K_{12} & K_{13} & K_{14} & K_{15} & K_{16} \\ & K_{22} & K_{23} & K_{24} & K_{25} & K_{26} \\ & & K_{33} & K_{34} & K_{35} & K_{36} \\ & & & K_{44} & K_{45} & K_{46} \\ & & & & K_{55} & K_{56} \\ & \text{symmetry} & & & & K_{66} \end{bmatrix}, \tag{A.10}$$

where its components are

$$\begin{aligned} K_{11} &= K_{44} = -K_{14} = -K_{41} = QL_e^{-1} c^2 + 12SL_e^{-3} s^2, \\ K_{22} &= K_{55} = -K_{25} = -K_{52} = QL_e^{-1} s^2 + 12SL_e^{-3} c^2, \\ K_{12} &= K_{21} = -K_{15} = -K_{51} = K_{45} = K_{54} = -K_{24} = -K_{42} = \\ &\qquad = (QL_e^{-1} - 12SL_e^{-3})\, sc, \\ K_{13} &= K_{31} = -K_{34} = -K_{43} = -RL_e^{-1} c - 6SL_e^{-2} s, \\ K_{23} &= K_{32} = -K_{35} = -K_{53} = -RL_e^{-1} s + 6SL_e^{-2} c, \\ K_{33} &= 2K_{36} = 2K_{63} = K_{66} = 4SL_e^{-1}, \end{aligned}$$

$$K_{16} = K_{61} = -K_{46} = -K_{64} = RL_e^{-1}\, c - 6SL_e^{-2}\, s,$$
$$K_{26} = K_{62} = -K_{56} = -K_{65} = RL_e^{-1}\, s - 6SL_e^{-2}\, c,$$
$$s = \sin\alpha, \qquad c = \cos\alpha.$$

After the displacements are solved, the internal forces are found as

$$\begin{aligned}
N_1 &= -N_2 = [(U_1-U_2)\, c+(V_1-V_2)\, s]\, QL_e^{-1} + (\phi_2-\phi_1)\, RL_e^{-1},\\
S_1 &= -S_2 = [(U_2-U_1)\, s+(V_2-V_1)\, c]\, 12SL_e^{-3} + (\phi_1+\phi_2)\, 6SL_e^{-2},\\
M_1 &= [(U_2-U_1)\, c+(V_2-V_1)\, s]\, RL_e^{-1} +\\
&\quad + [(U_2-U_1)\, s-(V_2-V_1)\, c]\, 6SL_e^{-2} + 2\,(2\phi_1+\phi_2)\, SL_e^{-1},\\
M_2 &= [(U_1-U_2)\, c-(V_2-V_1)\, s]\, RL_e^{-1} +\\
&\quad + [(U_2-U_1)\, s-(V_2-V_1)\, c]\, 6SL_e^{-2} + 2\,(\phi_1+2\phi_2)\, SL_e^{-1},
\end{aligned} \tag{A.11}$$

in which U, V, ϕ are the displacement components in global directions at nodes.

Reference

1. J. L. Batoz, G. S. Dhatt, *Incremental displacement algorithms for nonlinear problems*, Int. J. Num. Meth Eng., **14**, 1262–1265, 1979.
2. G. Powell, J. Simons, *Improved iteration strategy for nonlinear structures*, Int. J. Num. Meth. Eng., **17**, 1455–1467, 1981.
3. S. Pietruszczak, Z. Mróz, *Finite element analysis of deformation of strain softening materials*, Int. J. Num. Meth. Eng., **17**, 327–334, 1981.
4. Z. Waszczyszyn, C. Cichoń, *Methods of solving the nonlinear static stability structural behaviour using FEM* [in Polish], Conf. Recent Problems of Structural Stability, Janowice 1985.
5. P. G. Bergan, *Solution algorithms for nonlinear structural problems*, Comp. and Struct., **12**, 497, 1980.
6. B. -H. Kröplin, D. Dinkler, *A creep type strategy used for tracing the load path in elasto-plastic post-buckling analysis*, Comp. Meth. Appl. Mech. Enging., **32**, 365–376, 1982.
7. K. J. Bathe, E. N. Dvorkin, *On the automatic solution of nonlinear finite element equations*, Comp. and Struct., **17**, 871–879, 1983.
8. G. A. Wempner, *Discrete approximations related to nonlinear theories of solids*, Int. J. Solid. and Struct., **7**, 1581–1599, 1971.
9. E. Riks, *The application of Newton's method to the problem of elastic stability*, J. Appl. Mech., ASCE, **39**, 1060–1065, 1972.
10. E. Ramm, *Strategies for tracing the nonlinear response near limit points*, Nonlinear Finite Element Analysis in Structural Mechanics, Ruhr-Univ., pp. 13–89, ed. W. Wunderlich, E. Stein, K.-J. Bathe, Bochum, Germany 1979.
11. M. A. Crisfield, *A faster modified Newton-Raphson iteration*, Comp. Meth. Appl. Mech. Enging., **20**, 267–278, 1979.

12. M. A. CRIFIELD, *A fast incremental/iterative solution procedure that handles "snap-through"*, Comp. and Struct., **13**, 55–62, 1981.
13. M. A. CRIFIELD, *An arc-length method including line searches and accelerations*, Int. J. Num. Meth. Enging., **19**, 1269–1289, 1983.
14. M. A. CRISFIELD, *Snap-through and snap-back response in concrete structures and the dangers of under integration*, Int. J. Num. Meth. Enging., **22**, 751–767, 1986.
15. T. ŁODYGOWSKI, *Geometrically nonlinear elastic-plastic analysis of beams and frames* [in Polish], Arch. Inż. Ląd., **28**, 1–2, 79–97, 1982.
16. J. JIAN-JING, *Finite element techniques for static analysis of structures in reinforced concrete*, Chalmers Univ. of Technology, Goteborg, Publ. 83:2, Dept. Struct. Mech., Sweden 1983.
17. E. ONATE, J. OLIVER, G. BUGEDA, *Finite element analysis of the nonlinear response of concrete dams subjected to incremental loads*, FEMs in Nonlinear Problems, Trondheim, Norway, 1985.
18. Z. P. BAŽANT, T. B. BELYTSCHKO, T. P. CHANG, *Continuum theory for strain softening*, J. Enging. Mech., **110**, 1666–1692, Dec. 1984.
19. P. DAVALL, P. A. MENDIS, *Elastic-plastic-softening analysis of plane frames*, J. Struct. Enging., ASCE, 111, 871–888, Apr. 1984.
20. W. B. CRANSTON, *Tests on reinforced concrete frames. I. Pinned portal frames*, Tech. Rep., TRA/392, Cement and Concrete Association, London, Aug. 1965.
21. D. R. G. OWEN, E. HINTON, *Finite elements in plasticity. Theory and practice*, Pineridge Press Ltd., Swansea, U. K., 1980.
22. T. BELYTSCHKO, B. J. HSIEH, *Non-linear transient finite element analysis with convected coordinates*, Int. J. Num. Meth. Enging., 7, 255–271, 1973.

STRESZCZENIE

ANALIZA NUMERYCZNA BELEK I RAM Z MATERIAŁÓW OSŁABIAJĄCYCH SIĘ

Praca dotyczy analizy belek i ram ukazując osłabiające zachowanie się konstrukcji betonowych i żelbetowych. Efekt taki osiągnięto, zakładając dla betonu związki konstytutywne z osłabieniem zarówno w strefie ściskanej jak i rozciąganej. Do analizy numerycznej przyjęto model warstwowy elementu skończonego, w którym nie uwzględniono wpływu poślizgu na styku materiałów, zbrojenia i betonu. Mimo to otrzymane wyniki odwzorowują z zadowalającą dokładnością wyniki znanych doświadczeń laboratoryjnych. Zastosowano sformułowanie przyrostowe, a do sterowania procesem numerycznym tak zwaną metodę parametru ścieżki ("arc-length" — Crisfield) uwzględniającą równoczesną iterację wektora przyrostu przemieszczenia i parametru obciążenia.

Резюме

ЧИСЛЕННЫЙ АНАЛИЗ БАЛОК И РАМ ИЗ ОСЛАБЛИВАЮЩИХСЯ МАТЕРИАЛОВ

Работа касается анализа балок и рам, указывая на ослабливающееся поведение бетонных и железобетонных конструкций. Такой эффект достигнут, предполагая для бетона определяющие соотношения с ослаблением так в сжимаемой зоне, как и в рас-

тяжимаемой зоне. Для численного анализа принята слоистая модель конечного элемента, в которой не учтено влияние скольжения на контакте материалов, армировки и бетона. Несмотря на это полученные результаты отображают с достаточной точностью результаты известных лабораторных экспериментов. Применена формулировка в приростах, а для управления численным процессом применен так называемый метод параметра дорожки („arc-length" — Крисфильд), учитывающий интерацию вектора прироста перемещения и параметра нагружения.

TECHNICAL UNIVERSITY OF POZNAŃ, POZNAŃ.

Received August 28, 1987.